Progress in Oceanography 79 (2008) 278–289

Contents lists available at ScienceDirect

Progress in Oceanography

journal homepage: www.elsevier.com/locate/pocean

Impacts of Kelvin wave forcing in the Peru Humboldt Current system: Scenarios of spatial reorganizations from physics to fishers

Sophie Bertrand [a,b,c,*], Boris Dewitte [d,c], Jorge Tam [c], Erich Díaz [c], Arnaud Bertrand [b,c]

[a] University of Washington, School of Fisheries, Box 355640, Seattle, WA 98195, USA
[b] IRD, Centre de Recherche Halieutique Méditerranéenne et Tropicale, Avenue Jean Monnet, BP 171, 34203 Sète Cedex, France
[c] Instituto del Mar del Perú, CIMOBP, Esquina Gamarra y Gral. Valle s/n, Apartado 22, Callao, Lima, Peru
[d] IRD, UMR LEGOS, 14 Av. Edouard Belin, 31401 Toulouse Cedex 4, France

ARTICLE INFO

Article history:
Accepted 14 October 2008
Available online 21 October 2008

Keywords:
Climate forcing
Ecological scenarios
Fish distribution
Fishers' movements
Kelvin waves
Peru Humboldt Current system

ABSTRACT

Because climate change challenges the sustainability of important fish populations and the fisheries they support, we need to understand how large scale climatic forcing affects the functioning of marine ecosystems. In the Humboldt Current system (HCS), a main driver of climatic variability is coastally-trapped Kelvin waves (KWs), themselves originating as oceanic equatorial KWs. Here we (i) describe the spatial reorganizations of living organisms in the Humboldt coastal system as affected by oceanic KWs forcing, (ii) quantify the strength of the interactions between the physical and biological component dynamics of the system, (iii) formulate hypotheses on the processes which drive the redistributions of the organisms, and (iv) build scenarios of space occupation in the HCS under varying KW forcing. To address these questions we explore, through bivariate lagged correlations and multivariate statistics, the relationships between time series of oceanic KW amplitude (TAO mooring data and model-resolved baroclinic modes) and coastal Peruvian oceanographic data (SST, coastal upwelled waters extent), anchoveta spatial distribution (mean distance to the coast, spatial concentration of the biomass, mean depth of the schools), and fishing fleet statistics (trip duration, searching duration, number of fishing sets and catch per trip, features of the foraging trajectory as observed by satellite vessel monitoring system). Data sets span all or part of January 1983 to September 2006. The results show that the effects of oceanic KW forcing are significant in all the components of the coastal ecosystem, from oceanography to the behaviour of the top predators – fishers. This result provides evidence for a bottom-up transfer of the behaviours and spatial stucturing through the ecosystem. We propose that contrasting scenarios develop during the passage of upwelling versus downwelling KWs. From a predictive point of view, we show that KW amplitudes observed in the mid-Pacific can be used to forecast which system state will dominate the HCS over the next 2–6 months. Such predictions should be integrated in the Peruvian adaptive fishery management.

1. Introduction

Because climate change challenges the sustainability of important fish populations and the fisheries they support, we need to understand how large scale climate/ocean fluctuations affect the functioning of marine ecosystems (Stenseth et al., 2002; Edwards and Richardson, 2004; Worm and Myers, 2004; Burkett et al., 2005; Perry et al., 2005; Lehodey et al., 2006). The Humboldt Current upwelling system (HCS) provides an ideal opportunity to examine the effects of remote climate forcing on a coastal ecosystem as it is influenced by well-described multi-scale climatic forcing (seasonal, inter annual and decadal as well as local, regional and global dynamics, e.g. Chavez et al., 2003). Moreover, owing to the economic importance of the Peruvian anchovy or anchoveta (*Engraulis ringens*) fishery, the world largest monospecific fishery, many components of the ecosystem have been monitored for a relatively long period.

Understanding the response of marine ecosystems to large scale forcing is a difficult task, as climate variability has a stochastic component and biological responses are often non-linear (Hsieh et al., 2005). Such complexity can produce apparently chaotic dynamics at the regional scale, and the responses or evolution of regional systems can appear unpredictable (i.e. deterministic equations cannot describe or predict the succession of states). Still, system states having a high probability of occurrence, or scenarios (Link et al., 2002, use indifferently 'state', 'regime' and 'stanza'), can be statistically characterized (e.g. Knowlton, 2004).

One of the main sources of variability in the Humboldt Current system derives from the passage of coastally-trapped Kelvin waves

* Corresponding author. Address: IRD, Teruel 357, Miraflores, Casilla 18-1209, Lima 18, Peru. Tel.: +51 1 441 32 23.
E-mail address: Sophie.Bertrand@ird.fr (S. Bertrand).

0079-6611/$ - see front matter © 2008 Elsevier Ltd. All rights reserved.
doi:10.1016/j.pocean.2008.10.017

(KWs), themselves originating in the western and central Pacific as oceanic equatorial KWs (Pizarro et al., 2001). Equatorial KWs are large-amplitude, long-period waves which travel eastwards within the ocean along the equatorial wave guide (Delcroix et al., 2000). They are mostly forced in the central equatorial Pacific by variations in the wind and propagate at 1–3 m s^{-1}. According to the type of wind anomaly (easterlies or westerlies), an equatorial KW can rise (upwell) or deepen (downwell) the thermocline (often 10s of meters) and the sea surface height (centimeters). Because the equatorial thermocline is shallow, especially in the eastern Pacific, non-linear processes affect the speed and the vertical structure of the KW while propagating eastward. These changes in the KW properties can be analytically described by changes in the relative contribution to the overall signal of several linear components, the baroclinic modes (Dewitte et al., 1999). They are obtained by a mathematical decomposition of the KW signal and are the solutions of the linearized dynamical equations of movement on the vertical axis (Cane and Sarachick, 1976). Each of the baroclinic modes has distinct characteristics in terms of propagation, phase speed and meridional scale. As the KW propagate eastward, the relative contribution of each baroclinic mode in the global KW signal changes: KW energy projects more on the first baroclinic mode in the central Pacific, and on the third baroclinic mode close to South America coasts. Because the different baroclinic modes have different speeds and meridional scales (higher-order baroclinic modes propagate slower and are smaller in meridional extent), each may explain better the KW impact on different processes in the coastal ecosystem.

When equatorial KWs reach South America, part of their energy is deflected north and south along the coast where it is trapped by the earth's rotation (Coriolis) force, along the continental shelves or slope (Clarke, 1983, 1992). These coastally-trapped KWs impact the vertical structure of the isotherms along the coast and the location of the upwelling front. They also introduce energy for turbulent flow in the coastal ecosystem and are then likely to impact meso-scale activity and then the spatial structuring of many living communities. Downwelling KWs deepen the thermocline, making coastal upwelling 'inefficient' in terms of nutrient enrichment (brings to surface oceanic warm and low nutrient water; Barber and Chavez, 1983) and is associated with warm conditions (an El Niño-like scenario). Conversely, an upwelling KW raises the thermocline and allows coastal upwelling to bring cold and nutrient-rich water towards the surface. As a consequence, the cold coastal water (CCW) domain expands (a La Niña-like scenario).

The response of populations to climate forcing may be multidimensional: e.g. changes in abundance, in physiology of reproduction, in patterns of migration, in spatial distribution, etc. (e.g. Stenseth et al., 2002; Walther et al., 2002). The response in terms of organism abundance — the most commonly used metric — may be complex and delayed, as abundance is an indirect result of many interacting constraints: e.g. physical conditions, prey availability, reproductive success, competition, and others. Geographic distribution or organism movements are population features that can represent more direct responses to physical forcing (e.g. Perry et al., 2005; Bertrand et al., 2005). Climatic forcing primarily affects the physical habitat and, among other effects, may induce passive (plankton) or active (nekton) spatial redistributions of the living communities (Cotté and Simard, 2005; Croll et al., 2005; Fossheim et al., 2005; Bertrand et al., 2008). Patterns of space occupation, whether for individuals or populations (Margalef, 1979), control ecological interactions such as predation, competition and reproduction which, in turn, feed back to population abundance (e.g. Frontier et al., 2004). Analyzing the spatial redistributions of populations in response to climatic forcing may provide a valuable intermediate step towards understanding changes in population abundance (Keitt et al., 2002).

The purpose of this paper is to define ecological scenarios for the Peruvian coastal ecosystem under varying oceanic equatorial KW forcing. To address these questions, we explore through bivariate lagged correlations and multivariate statistics the relationships between a variety of time series of oceanic KW amplitude (TAO mooring data and model-resolved baroclinic modes) and coastal Peruvian oceanographic data (SST, coastal upwelled waters extent), anchoveta spatial distribution (mean distance to the coast, spatial concentration of the biomass, mean depth of the schools), and fishing fleet statistics (trip duration, searching duration, number of fishing sets and catch per trip, features of the foraging trajectory as observed by satellite vessel monitoring system). Data sets span all or part of January 1983 to September 2006. In particular we (i) describe the spatial reorganizations in the coastal HCS as affected by oceanic KWs forcing, (ii) quantify the strength of the interactions between the dynamics of the physical and biological components of the system, (iii) formulate hypotheses on the processes driving the redistributions of the organisms, and (iv) synthesize the scenarios of space occupation in the HCS under varying KWs forcing.

2. Materials and methods

To quantify oceanic KW forcing, Peruvian coastal oceanography, anchoveta distribution and the foraging behaviour of fishermen, we gathered a large variety of field measurements and model outputs (Table 1). The different data sets were collected over different periods, but always between January 1983 and September 2006 (Table 1, Figs. 1 and 2).

2.1. KW forcing

A proxy for Kelvin wave activity in the equatorial Pacific can be observed through the depth of the 20 °C isotherm (D20) as measured by the TAO/TRITON moorings (Tropical Atmosphere/Ocean, http://www.pmel.noaa.gov/tao/data_deliv/deliv.html). D20 is a robust proxy for KW activity; nevertheless the signal contains also a contribution from reflected Rossby wave (generated by the reflection of part of the KW energy when they hit the South America shore). We analyzed the times series provided by the moorings located at 0°N–95°W and 0°N–155°W. The 95°W mooring was chosen as closest to the coast and the HCS. Data were available from January 1983 to September 2006, with some gaps. The 155°W mooring was chosen as representative of the mid-Pacific, closer to the location of the initiation of the KWs. Data were available from August 1991 to September 2006.

Because the different baroclinic modes of each KW may impact different processes in the coastal ecosystem, it is relevant to analyze their respective contribution to coastal ecosystem variability. Following earlier works (Dewitte et al., 1999, 2003), we consider the first three baroclinic modes (referred hereafter as ak1, ak2 and ak3 for the first three baroclinic modes, respectively); these are the most energetic propagating modes. Their contribution to the total KW amplitude can be resolved from observational data (e.g. wind) input into an ocean model either through direct forcing or through assimilation. For this work we used two model output products.

First, we used output from the simple ocean data assimilation reanalysis of ocean climate variability (SODA, Carton et al., 2000). SODA is an ocean reanalysis product that combines observations (historical archive of hydrographical profiles supplemented by ship intake measurements, moored hydrographical observations, and remotely sensed SST and sea level) with an ocean general circulation model (Geophysical Fluid Dynamics Laboratory MOM2 physics). It creates a grid dataset of ocean features (e.g. temperatures,

Table 1
Acronym, description, data type and time series available for each parameter used in the analysis.

Variable acronym	Description	Data type	Time series available
ak1 SODA 85°W ak2 SODA 85°W ak3 SODA 85°W	First, second and third KW baroclinic mode calculated from SODA at 85°W	Ocean model outputs	January 1983–December 2004
∑ak SODA 85°W	Total KW amplitude from SODA at 85°W (sum of the three first baroclinic modes)		
ak1 SODA 160°W ak2 SODA 160°W ak3 SODA 160°W	First, second and third KW baroclinic mode calculated from SODA at 160°W		
∑ak SODA 160°W	Total KW amplitude from SODA at 160°W (sum of the three first baroclinic modes)		
ak1 LM 80°W ak2 LM 80°W ak3 LM 80°W	First, second and third KW baroclinic mode calculated from linear model at 80°W		January 1983–September 2006
∑ak LM 80°W	Total KW amplitude from linear model at 80°W (sum of the three first baroclinic modes)		
ak1 LM 160°W ak2 LM 160°W ak3 LM 160°W	First, second and third KW baroclinic mode calculated from linear model at 160°W		
∑ak LM 160°W	Total KW amplitude from linear model at 160°W (sum of the three first baroclinic modes)		
D20 95°W D20 155°W	20 °C isotherm depth at 95°W and 155°W	TAO moorings	January 1983–September 2006, with gaps August 1991–September 2006
SST	Monthly averaged sea surface temperature off Chicama	IMARPE specific sampling	January 1983–September 2006
DC_{CCW}	Mean distance to the coast of the cold coastal waters centroïd	IMARPE acoustic surveys	October 83–December 2005 Discrete data
MSD	Mean schools depth of anchoveta		
DC_{anch}	Anchoveta mean distance to the coast		
ISO	Percentage of positive (anchoveta $s_A > 0$) elementary sampling distance units		
TD	Monthly averaged travel duration	IMARPE observers at sea aboard fishing vessels	December 1995–September 2006 with gaps (fishery closed)
SD	Monthly averaged searching duration		
NFS	Monthly averaged number of fishing sets		
TC	Monthly averaged trip catch		
μ	Sinuosity and diffusion index from random walk modelling	Model output from satellite fishing vessel monitoring system	November 1999–June 2006, with gaps (fishery closed)

ocean salinities, ocean currents) from which the Kelvin wave contribution to the sea level anomaly for the first three baroclinic modes can be derived (see Dewitte et al., 1999 for more details on the method). To cover 1983–2004, we used two SODA reanalysis experiments which differ by the atmospheric forcing used (see Carton and Giese, 2008): the basic reanalysis, SODA1.4.2, spans the 44 year period from 1958 to 2001; a second reanalysis experiment, SODA1.4.3, spans the period of QuikSCAT scatterometer winds from 2000 to 2004. Carton and Giese (2008) have shown that the agreement between the two products over the 2-year overlapping period (2000–2001) is good. We then built composite time series of monthly mean sea level anomaly originating from the first three baroclinic modes (ak1 SODA, ak2 SODA and ak3 SODA), spanning 1983–2004.

Second, the contribution of these three baroclinic modes was derived from linear model ('LM'; Dewitte et al., 2002) simulations forced by *in situ* (FSU) and satellite-derived (ERS1 and 2 and QuickSCAT) winds to produce time series spanning January 1983-September 2006 (ak1 LM, ak2 LM and ak3 LM). The LM assumptions are less realistic than SODA (it does not include thermocline dynamics), but this model is much less computationally intensive and allows to generate longer time series of baroclinic modes amplitude from wind product only. As a consequence, LM spans the entire time series from January 1983 to September 2006.

2.2. Coastal oceanography

We used two indicators to describe the physical state of the coastal ocean off Peru. First, the monthly averaged sea surface temperature (SST) off Chicama (collected by IMARPE) presents a long and complete time series and was used as a proxy of the average coastal temperature (Gutiérrez et al., 2007). Second, we estimated offshore extent of the cold coastal waters (CCW) resulting from coastal upwelling. Water masses including CCW were defined with an algorithm using temperature, salinity, season and latitude data collected at regular stations during the scientific surveys performed by IMARPE (see next paragraph and Swartzman et al., 2008 for details). We calculated the mean distance to the coast of the CCW centroid (DCccw) and take this distance to estimate the range of extension or width of the CCW.

2.3. Anchoveta distribution

In Peru, annual acoustic surveys of fish population distribution and abundance have been conducted since 1983 by IMARPE. Surveys occupied on/offshore parallel transects averaging 90 nautical miles (167 km) offshore, with inter-transect distance varying between 14 and 16 nautical miles (26–30 km). Acoustic data were collected by Simrad echosounders (EK, EKS, EK400 before 1995, and EY500, EK500 thereafter, except an EK60 was used 2001–2005 in one vessel). Calibration and intercalibration of the echosounders were undertaken before each survey according to Foote et al. (1987). The acoustic nautical area scattering coefficient (s_A), an index of fish abundance, was recorded in each geo-referenced elementary sampling distance unit (ESDU) of 2 n.mi. (1983–1993) or 1 n.mi. (1994–2006). Anchoveta were identified in the acoustic data with trawl samples. From the acoustic data, we extracted for each survey three metrics of anchoveta distribution:

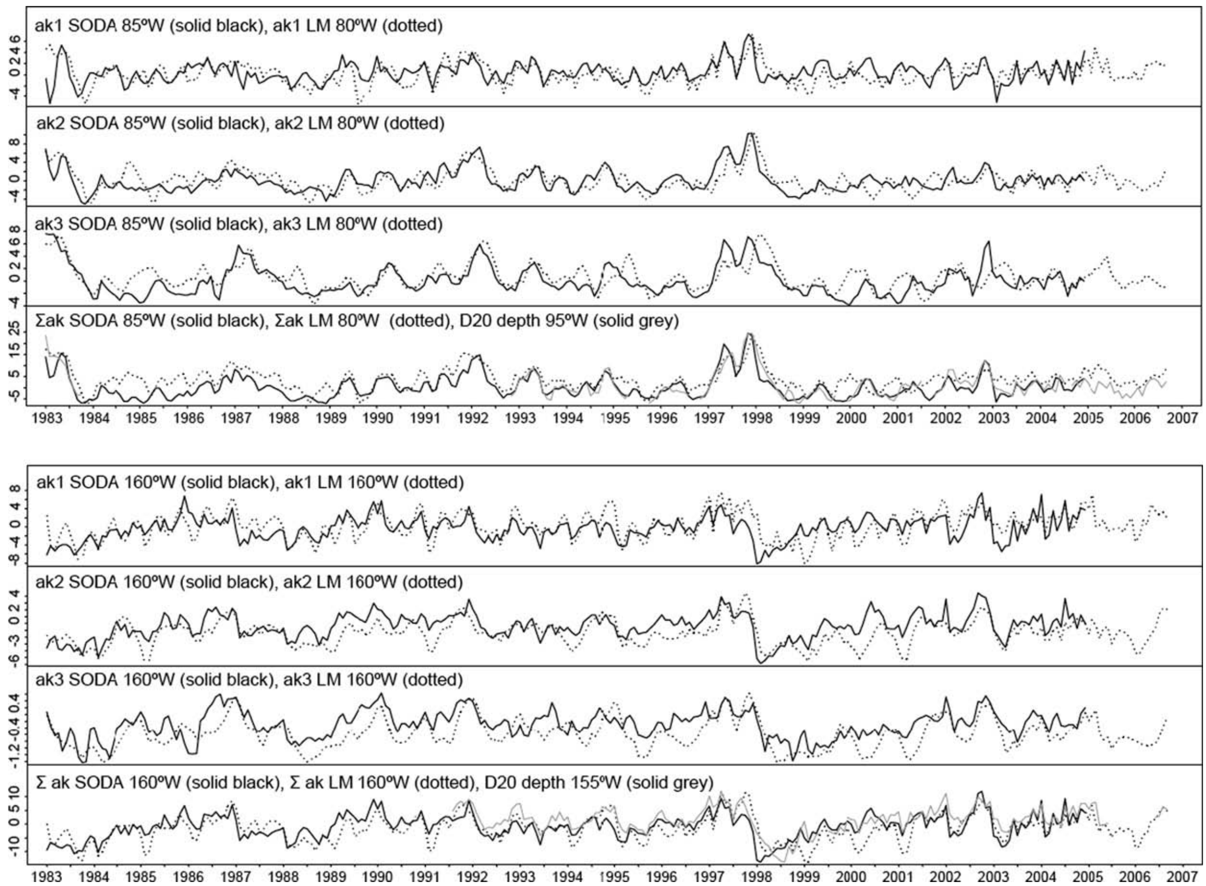

Fig. 1. Time series for the variables describing the Kelvin wave amplitude: first three baroclinic modes (ak1, ak2, ak3) and their sum ($\sum$ak) from SODA and linear model (LM) outputs, and depth of the 20 °C isotherm from TAO moorings (D20).

(i) mean distance to the coast (DCanch; see Swartzman et al., 2008); (ii) an index of spatial occupation (ISO) of fish biomass defined as the percentage of positive (anchoveta $s_A > 0$) ESDU (Bertrand et al., 2004a); and (iii) the mean depth of anchoveta schools (MSD).

2.4. Fishing activity

The description of fishing activity relies on two observation platforms. First we used information collected daily by an onboard IMARPE observers program running since 1996. When the fishery is open, about 25 vessels carry an observer (Bertrand et al., 2004c). Observers record the trip duration (TD), the searching duration (SD), the number of times the net was set (NFS), and the trip catch (TC). These variables, collected for each fishing trip, were averaged by month. Second, we used an index (μ) describing the movements of fishing vessels when foraging for anchoveta (Bertrand et al., 2005, 2007). This index is derived from a Lévy random walk modelling of the fishing trip trajectories as observed by a satellite vessel monitoring system (VMS). This index, whose values range between 1 and 3, describes both the sinuosity and the area explored (diffusion) by a vessel trajectory. When μ is high, the search is close to random, with high sinuosity and low diffusion. In others terms, time allocated to searching and fishing is high and time allocated to steaming is low. When μ is low, the search is close to ballistic or directed, with low sinuosity and high diffusion (Bertrand et al., 2005, 2007). In that case, time allocated to steaming, between fish aggregations, is higher. Data from observers at sea are available from December 1995 to September 2006; data from VMS from November 1999 to September 2006.

2.5. KW impact on coastal ecosystem dynamics: data analysis

We used 18 variables to describe the characteristics of the KWs and their baroclinic modes: (i) the amplitude of baroclinic modes ak1, ak2, ak3, and their sum ($\sum$, showing the global amplitude of the wave and therefore the amplitude of the sea level anomaly) as estimated from SODA at 85°W and 160°W and from LM at 80°W and 160°W, and (ii) D20 at 95°W and 155°W. In addition, 'coastal ecosystem' dynamics were described by 10 variables as defined above: SST, DCccw, MSD, DCanch, ISO, TD, SD, NFS, TC and μ.

2.5.1. Bivariate correlations

The relationships between KW forcing and coastal ecosystem dynamics were explored through two different statistical approaches. First, we used bivariate Pearson correlation tests to quantify the strength of the relationship between each KW baroclinic mode and each coastal ecosystem variable and to identify if these coastal ecosystem variables responded (with delay) to the KW forcing. Each of the coastal ecosystem variables was correlated with 1–4 months lags to SODA at 85°W, LM at 80°W and D20 at 95°W and with 1–6 months lags to SODA and LM at 160°W and D20 at 155°W. Because many variables were only available on a discrete basis (acoustic surveys) and others had a significant number of missing data, no systematic treatment could remove seasonality or autocorrelation. This is not a serious problem for several reasons. First, the raw time series (Figs. 1 and 2) show that, in general, the seasonal cycle is not strong enough to blur lower frequency signals (El Niño 1997–98 event for instance). Second, according to Pyper and Peterman (1998), removing autocorrelation

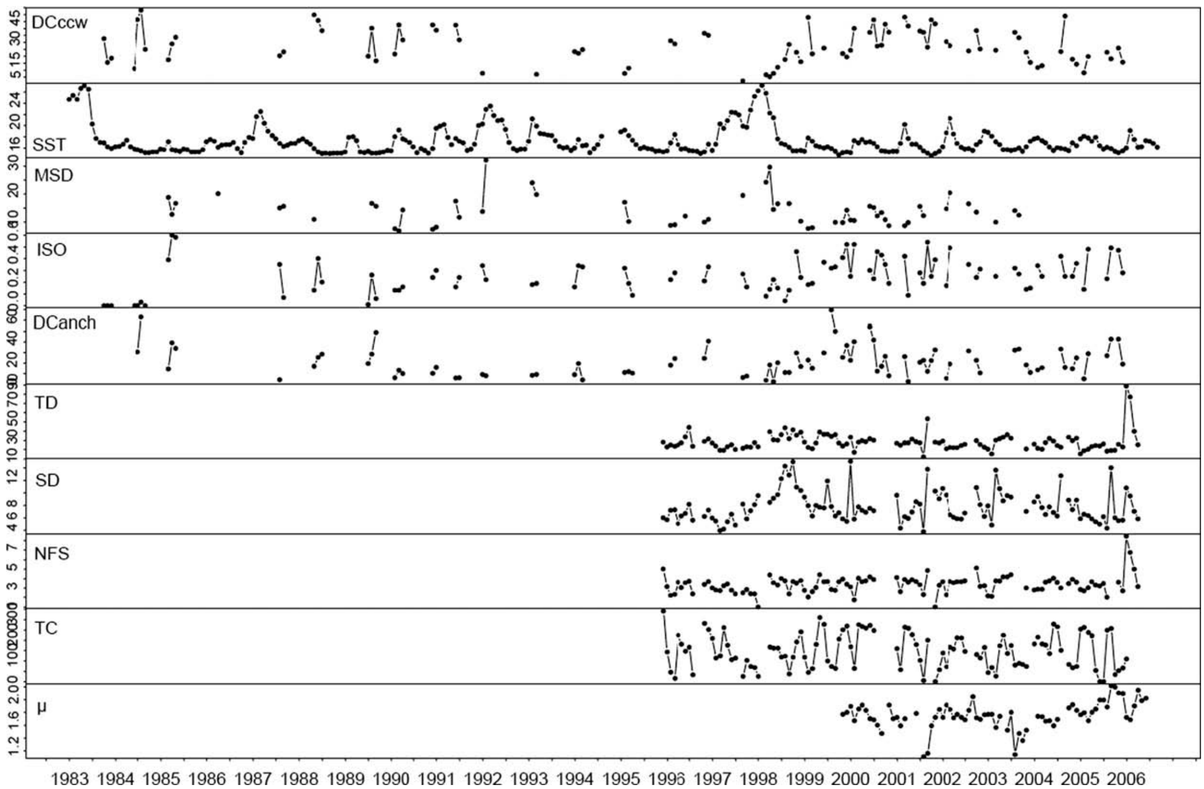

Fig. 2. Time series for the variables describing the Peruvian coastal ecosystem dynamics: mean distance to the coast of the cold coastal waters (DCccw), sea surface temperature off Chicama (SST), mean depth of anchoveta schools (MSD), spatial concentration of anchoveta biomass (ISO), mean distance to the coast of anchoveta (DCanch), mean fishing trip duration (TD), mean searching duration (SD), mean number of fishing sets by trip (NFS), mean catch by trip (TC), and the synthetic index describing fishing trip trajectories (μ).

(for example by 'prewhitening', by first differencing) makes implicit assumptions that low-frequency variability is unimportant or may add noise to the time series. The same authors propose an alternative method to account for autocorrelation, which consists of reducing the degrees of freedom with a modified Chelton (1984) method, estimating a lower critical p-value. However, because many of our variables have missing data, we could not estimate the autocorrelation functions required for this method, so we simply considered test results with $p < 0.01$ as significant. As we performed a large number of correlations (1080), we applied the false discovery rate (FDR) multitest correction to avoid inflating Type I error (Benjamini and Hochberg, 1995). For this test, p-values of the n tests are ranked in ascending order. The null hypothesis is rejected for all the tests of rank j inferior to k, k being the rank satisfying:

$$p_k <= k \cdot \alpha \cdot n^{-1} \quad (1)$$

Finally, the overall adequacy of linear modelling (an underlying assumption for a parametric bivariate correlation test) was checked using non-parametric cubic spline smoothers with S-Plus (Insightful Corporation, Seattle, WA, USA).

2.5.2. Multivariate statistical approach

Second, to identify the major scenarios of the coastal ecosystem and to examine its multivariate trajectory in the phase-space of the KW forcing, we completed the investigation through multivariate statistics. We built a principal component analysis (PCA, e.g. Lebart et al., 2000) with the KW forcing variables (ak1, ak2, ak3, SODA 85°W and LM 80°W, D20 at 95°W) as continuous active variables. We projected all the other variables (illustrative) on the factorial space built by the continuous variables to investigate the effect of KW forcing on the coastal ecosystem dynamics. To facilitate the interpretation and to search for non-linear processes, we categorised each illustrative variable in three modalities: low (1), medium (2) and high (3). We finally projected the 285 study months on the factorial space to identify the main scenarios for this ecosystem and to follow the multivariate trajectory of the system through time (Link et al., 2002).

3. Results

Raw time series for the 18 metrics describing the KWs forcing and the 10 metrics describing the coastal ecosystem dynamics are presented in Figs. 1 and 2, respectively. These figures highlight the different time span covered by each of these metrics and clearly show extreme events such as the El Niño of 1997–98.

3.1. Correlations between TAO observations and models outputs

Table 2 synthesises results of correlation tests performed between the data describing the KWs: D20 at 95°W and 155°W, and the corresponding outputs of SODA and LM. SODA output data ($\sum$ak SODA) were globally more correlated to TAO observations (D20; $\rho = 0.90$ and $\rho = 0.80$ for the eastern and western time series, respectively) than LM output ($\sum$ak LM, $\rho = 0.79$ and $\rho = 0.77$ for the eastern and western time series, respectively). This result is consistent with the more realistic assumptions made by SODA on the ocean structure compared with LM (no thermocline dynamics in LM).

Correlation between SODA and LM outputs was approximately the same for the eastern and western time series for ak2 ($\rho = 0.66$ and $\rho = 0.67$, respectively) and ak3 ($\rho = 0.69$ and $\rho = 0.68$, respectively). There was more difference for the first baroclinic mode between the eastern and western time series (ak1;

Table 2
Equatorial KWs forcing, correlations between observations and models outputs: depth of the 20 °C isotherm from TAO moorings (D20), first three baroclinic modes (ak1, ak2, ak3) and their sum (∑) from SODA and the linear model (LM).

Type of test	Variable 1	Variable 2	ρ Pearson	p-Value	df
Correlations between models outputs and observations	∑ak SODA 85°W	D20 depth 95°W	0.90	0	96
	∑ak LM 80°W	D20 depth 95°W	0.79	0	115
	∑ak SODA 160°W	D20 depth 155°W	0.80	0	158
	∑ak LM 160°W	D20 depth 155°W	0.77	0	168
Correlations between SODA outputs and linear model outputs	ak1 SODA 85°W	ak1 LM 80°W	0.48	0	262
	ak2 SODA 85°W	ak2 LM 80°W	0.66	0	262
	ak3 SODA 85°W	ak3 LM 80°W	0.69	0	262
	∑ak SODA 85°W	∑ak LM 80°W	0.76	0	262
	ak1 SODA 160°W	ak1 LM 160°W	0.58	0	262
	ak2 SODA 160°W	ak2 LM 160°W	0.67	0	262
	ak3 SODA 160°W	ak3 LM 160°W	0.68	0	262
	∑ak SODA 160°W	∑ak LM 160°W	0.67	0	262

$\rho = 0.48$ and $\rho = 0.58$ for the eastern and western time series, respectively). The difference between the two models is reduced in the oceanic domain (western time series) where non linear processes are less important. The correlation between SODA and LM was lower for ak1 than for ak2 and ak3. The LM estimate of the first KW baroclinic mode (ak1) also contains over-energetic sub-seasonal variability due to the overestimation of reflection of the Rossby waves at the western boundary (idealized boundaries in LM versus realistic coastline and topography for the SODA model; and simplified formulation for friction in LM).

3.2. Bivariate correlations

Correlations were explored between the 18 metrics describing the KW forcing and the 10 metrics describing the Peruvian coastal ecosystem dynamics, these being lagged either 1–4 or 1–6 months lags for the eastern and western KW forcing, respectively. A total of 414 of 1080 correlations were significant (at $p < 0.01$) after FDR multitest correction. The linear assumption underlying those correlations (see Fig. 3 for examples of bivariate relationships) was acceptable for most of the variables.

Results of significant correlations are synthesised for the eastern KW time series (D20 95°W, SODA 85°W and LM 80°W) in Table 3, and western KW time series (D20 155°W, SODA 160°W and LM 160°W) in Table 4. Only those results corresponding to the baroclinic mode and the time lag maximizing the correlation for each time series are presented. In most cases, significant correlations were also obtained for close lags or modes. Overall trends for each dependent variable are symbolised in the column 3 of Tables 3 and 4.

A downwelling KW near the coast [i.e. a high positive anomaly for the D20 depth at 95°W and high positive anomaly of the sea surface height from SODA (85°W) or LM (80°W)] leads to (Table 3): (i) an increase in SST (max ρ: 1 month lag with D20); (ii) a decrease in the extent of cold coastal waters (DCccw, max ρ: 3 months lag with D20 and ∑ak LM); (iii) a deepening of the mean depth of anchoveta schools (MSD, max ρ: 1 month lag with D20); (iv) a reduction in the extent of anchoveta distribution (DCanch, max ρ: no lag with ak3 SODA); (v) an increased spatial concentration of anchoveta biomass (lower ISO, max ρ: 3 months lag with ak3 SODA); (vi) a decrease in the mean fishing trip duration and the time allocated to searching by fishers (TD and SD, max ρ: no lag with ak2 SODA); (vii) a decrease in the mean number of fishing sets per trip (NFS, max ρ: 2 months lag with ak1 SODA); (viii) a decrease in the total catch per trip (TC, max ρ: 3 months lag with ak3 SODA); and (ix) an increase in the sinuosity by fishing trip trajectories (μ, max ρ: 1 month lag with ak2 LM). The strength of these correlations (mean ρ values) generally decreases from the coastal oceanography indices to the fishing activity indices, probably illustrating the increasing complexity or indirect nature relations between the physical forcing and the impacted processes. The trends obtained under an upwelling KW forcing are symmetrically opposite.

A downwelling KW detected far from the coast (155–160°W) leads to similar trends at the coast (85–95°W) but with longer lags (Table 4). The only difference in the overall trends is a decrease in spatial concentration of anchoveta (ISO positive). This result should be considered with caution because only one correlation was significant for ISO. As for the eastern time series, the situation is symmetrically opposite under an upwelling KW forcing.

3.3. Multivariate statistics

The first two factors of the PCA built with ak1, ak2, ak3 from SODA at 85° W and from LM at 80°W and D20 depth from TAO at 95° W represent 63.7% and 12.9% of the total variance, respectively (Fig. 4a). The first factor can be interpreted as a global descriptor of the KW signal and sets the warm events (left panel of the multifactorial plane corresponds to downwelling KWs associated with elevated sea surface and deepened thermocline) against the cold events (right panel of the multifactorial plane corresponds to upwelling KWs associated with reduced sea level and shallowed thermocline). The second factor, which explains much less variance than factor 1, sets mainly the baroclinic modes of higher order (ak3) against the ones of lower order (ak1).

The projections of the modalities of the 10 variables describing the dynamics in the Peruvian coastal ecosystem on this space (Fig. 4b; categorised in three modalities, with time lags maximizing their coordinates on the first factor) shows generally similar patterns to those described by bivariate correlations (Tables 3 and 4), with slightly different lag periods. A warm event, characterized by a downwelling KW (left panel of the multifactorial space) is associated with: (i) an increased SST (modality 3, 1 month lag); (ii) a lower mean distance to the coast of the coastal cold water (CCW; modality 1, 3 months lag); (iii) a increased mean school depth (MSD, modality 3, 3 months lag); (iv) a reduced mean distance to the coast of anchoveta (DCanch, modality 1, no lag); (v) an increased spatial concentration of the fish biomass (ISO, modality 1, 1 month lag); (vi) low fishing trip duration (TD, modalities 1 and 2, no lag); (vii) low searching duration (SD, modalities 1 and 2, 1 month lag); (viii) low number of fishing sets (NFS, modality 1, 1 month lag); (ix) low total catches (TC, modalities 1 and 2, 3 months lag); and (x) fishing trip trajectories characterized by higher sinuosity and lower diffusion (μ, modalities 2 and 3, no month lag). The situation for a cold event, characterized by an upwelling KW forcing, is symmetrically opposite.

The projection of the 285 study months on this multivariate space shows the ecosystem trajectory in the phase-space of the oceanic KW forcing (Fig. 5). A main cloud of points is projected on the central-right part of the first factorial plane and represents the dominant 'cold' ecological scenario where the Peruvian ecosystem has mainly laid for the study period. Apart from this cloud a series of isolated points lie on the left part of the factorial plane. These represent El Niño warm extreme events. When these points are linked through their succession in time (Fig. 5), the trajectories over three El Niño's: 1982–83, 1991–92, 1997–98) are revealed.

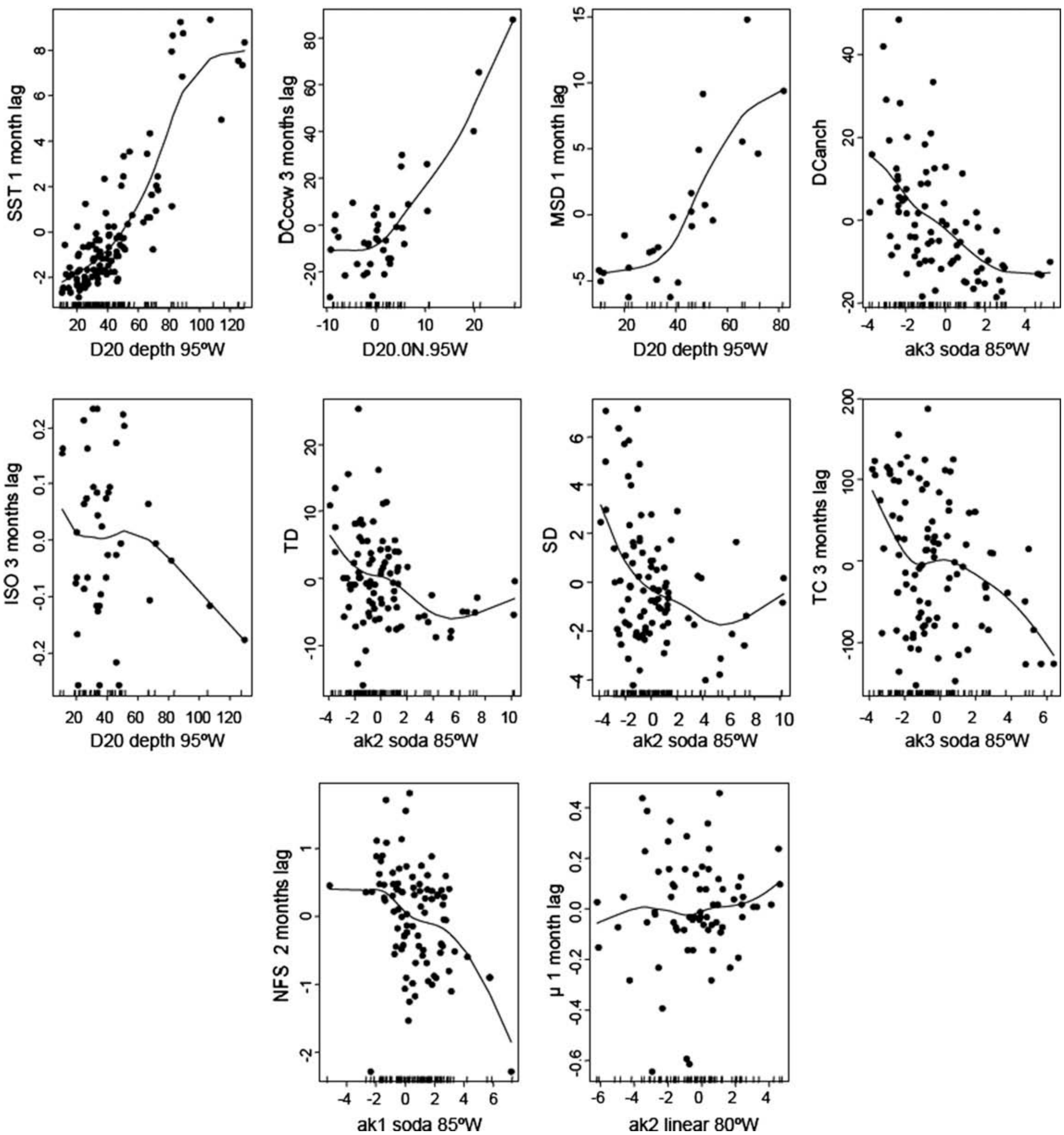

Fig. 3. Examples of non-parametric cubic Spline smoothers applied to the bivariate relationships that maximized the correlation between oceanic KWs signal (D20 at 95°W, SODA 85°W and linear model 80°W) and metrics describing the Peruvian coastal ecosystem dynamics.

Table 3
Synthesis of the bivariate Pearson correlations between the eastern KWs indexes (D20 at 95°W, SODA at 85°W and linear model (LM) at 80°W) and the metrics describing the Peruvian coastal dynamics, each of these being lagged up to 4 months: sea surface temperature off Chicama (SST), mean distance to the coast of the cold coastal waters (DCccw), mean depth of anchoveta schools (MSD), mean distance to the coast of anchoveta (DCanch), index of surface occupation by anchoveta (ISO, lower is ISO, higher is the spatial concentration of anchoveta), mean total duration of the fishing trips (TD), mean time allocated to search for fish (SD), mean number of fishing sets (NFS), mean catch by trip (TC), and an synthetic index of the fishing vessel trajectory (μ). All these results were significant at $p < 0.01$ after multitest correction. Only the statistical results corresponding to the baroclinic mode and the time lag maximizing the correlation for each parameter are presented. In most of cases, close significant results were obtained for a close time lag and/or mode. These overall results are synthesised in the column presenting the general trend of the correlations for each dependent variable.

Impact of oceanic KWs forcing on		General trend	D20 at 95°W			SODA 85°W				LM 80°W			
			ρ	df	Lag	KW baroclinic mode	ρ	df	Lag	KW baroclinic mode	ρ	df	Lag
Peruvian coastal oceanography	SST	↗	0.85	111	1	ak3	0.80	258	0	ak3	0.74	279	0
	DCccw	↘	−0.54	38	3	ak3	−0.51	80	2	$\sum$ak	−0.54	85	3
Anchoveta distribution	MSD	↗	0.80	22	1	ak3	0.53	56	1	$\sum$ak	0.65	56	2
	DCanch	↘	−0.50	37	1	ak3	−0.55	78	0	ak2	−0.46	84	0
	ISO	↘	–	–	–	ak3	−0.32	87	3	–	–	–	–
Fishing fleet behaviour	TD	↘	–	–	–	ak2	−0.34	89	0	–	–	–	–
	SD	↘	–	–	–	ak2	−0.31	89	0	–	–	–	–
	NFS	↘	−0.35	61	3	ak1	−0.40	91	2	ak2	−0.28	103	0
	TC	↘	–	–	–	ak3	−0.35	95	3	ak2	−0.26	105	0
	μ	↗	–	–	–	–	–	–	–	ak3	0.32	69	1

Table 4
Synthesis of the bivariate Pearson correlations between the western KWs indexes (D20 at 155°W, SODA at 160°W and linear model (LM) at 160°W) and the metrics describing the Peruvian coastal dynamics, each of these being lagged up to 4 months: sea surface temperature off Chicama (SST), mean distance to the coast of the cold coastal waters (DCcw), mean depth of anchoveta schools (MSD), mean distance to the coast of anchoveta (DCanch), index of surface occupation by anchoveta (ISO, lower is ISO, higher is the spatial concentration of anchoveta), mean total duration of the fishing trips (TD), mean time allocated to search for fish (SD), mean number of fishing sets (NFS), mean catch by trip (TC), and an synthetic index of the fishing vessel trajectory (μ). All these results were significant at $p < 0.01$ after multitest correction. Only the statistical results corresponding to the baroclinic mode and the time lag (in months) maximising the correlation for each parameter are presented. In most of cases, close significant results were obtained for a close time lag and/or mode. These overall results are synthesised in the column presenting the general trend of the correlations for each dependent variable.

Impact of oceanic KWs forcing on		General trend	D20 at 155°W			SODA 160°W				LM 160°W			
			ρ	df	Lag	Baroclinic KW mode	ρ	df	Lag	Baroclinic KW mode	ρ	df	Lag
Peruvian coastal oceanography	SST	↗	0.46	160	4	ak3	0.39	258	6	ak3	0.62	276	3
	DCccw	↘	–	–	–	–	–	–	–	ak2	−0.42	85	5
Anchoveta distribution	MSD	↗	0.51	38	6	ak3	0.41	56	5	ak3	0.53	56	5
	DCanch	↘	−0.33	63	5	ak3	−0.44	80	5	ak3	−0.45	84	2
	ISO	↗	–	–	–	∑ ak	0.28	86	2	–	–	–	–
Fishing fleet behaviour	TD	↘	−0.57	96	2	∑ak	−0.48	92	3	ak3	−0.33	105	2
	SD	↘	−0.48	96	2	ak1	−0.39	94	5	ak1	−0.26	105	3
	NFS	↘	−0.28	96	2	∑ak	−0.32	92	3	ak2	-0.32	103	3
	TC	↘	–	–	–	–	–	–	–	ak2	−0.34	105	2
	μ	↗	–	–	–	–	–	–	–	ak2	0.35	69	6

The difference in trajectories illustrates the difference in magnitude of the El Niño events (lower for the event of 1991–92).

4. Discussion

Our main objective has been to describe how large scale oceanic forcing via Kelvin waves (KWs) affects the coastal Peruvian ecosystem. How is the global energy of a basin-scale process released when arriving at the coast? It is usually admitted that the arrival of oceanic upwelling or downwelling KWs may have two types of consequences in the coastal domain. First, by changing the thermocline depth, KWs increase or decrease nutrient supply to the surface via upwelling (Barber and Chavez, 1983). If the upwelling pump is less efficient, the consequence is a reduction of the extent of rich and cold coastal surface waters and as a consequence, an apparent intrusion of warm oceanic waters. Additionally, passage of coastally-trapped KWs modifies the cross-shore temperature gradient (upwelling front), may change the stability of the upwelling currents (Morel et al., 2007) and can trigger extra-tropical Rossby waves that radiate offshore. Near the upwelling front, KWs induce meso-scale mixing and diffusion.

This work quantifies the direction and the strength of interaction between oceanic KW forcing and coastal ecosystem dynamics. SODA's underlying assumptions are more realistic than those of LM and in better agreement with TAO observations (D20). However when considering the western oceanic forcing signal, the LM was almost as good as SODA and even better correlated with the coastal parameters (Table 4). The LM time series also identified a correlation between KWs and the spatial behaviour of fishers (μ). This result is probably due to a better coherence between the time series (data allowing μ estimation were only available from 1999). Despite these minor inconsistencies between KWs descriptors, the two statistical approaches — bivariate lagged correlations and multivariate statistics — produced coherent and complementary results.

We could portray contrasting coastal scenarios according to the nature of the oceanic KW forcing (Fig. 6). A downwelling KW, by depressing the thermocline, makes that coastal upwelling brings to surface warmer, low nutrient waters (Barber and Chavez, 1983). Then, the extent of cold and nutrient-rich waters, CCW, is reduced (↘ DCccw), and sea surface temperature increase (↗SST) in the coastal domain. With these changes anchoveta tend to distribute (i) closer to the coast (↘ DCanch), remaining in the CCW (Bertrand et al., 2004b; Swartzman et al., 2008), and (ii) deeper in the water column (↗ MSD) beneath the warm and less productive surface waters (e.g. Arntz and Fahrbach, 1996). Under these conditions anchoveta are concentrated in space (↘ ISO, see Gutiérrez et al., 2007) and the time needed by fishers to find anchoveta aggregations is reduced (↘ SD) and fishing trips are briefer (↘ TD). The number of fishing sets by trip also decreases (↘ NSF) as does the catch per trip (↘ TC). When fish are concentrated in the very coastal fringe the decreased TC seems surprising but may have several explanations: (i) when operating close to the coast, fishers offload more frequently, even when only partly loaded; (ii) anchoveta may be less available to the industrial fleet which, by law, cannot fish nearshore (<5 n.mi.); (iii) anchoveta may move too deep to be available to the purse seine (Bertrand et al., 2004b). Finally, the trajectories followed by the fishing vessels are more sinuous, random-like, and explore smaller areas (↗ μ). This 'Brownian'-like motion occurs because the ships do not need to steam offshore (directed travel) and between clusters when anchoveta are concentrated near the coast in highly contagious aggregations (Clark, 1976; Bertrand et al., 2005). The scenario under the arrival of an upwelling KW is symmetrically opposite to what was described for downwelling KWs (Fig. 5).

Several of these patterns have been described previously (e.g. McPhaden, 1999; Escribano et al., 2004), but the contribution of oceanic KW forcing to the changes in the coastal ecosystem had not been quantified. This work shows that the effect of large scale oceanic KW forcing is detectable and significant in the spatial organization of the ecosystem, including anchoveta and one of their top predators, man. This is an evidence for a bottom-up transfer of the behaviours and spatial structuring (Frontier, 1987; Russel et al., 1992): physics structures the oceanscape and drives the distribution of particles and passive organisms (plankton); then, because living organisms have to meet their prey, they tend to track their distribution (e.g. Frontier et al., 2004) and by the succession of predator–prey relationships, the spatial structuring originally driven by physical forcing tends to be transmitted along the trophic levels of the ecosystem (Fig. 7). Attenuation of the correlations from the oceanographic descriptors (most correlations being in the order of 0.65) to the fishery descriptors (most correlations being in the order of 0.35) reflects the increasing complexity of the factors driving the spatial distributions from physics (water masses redistribution obeying fluid mechanics rules) to living organisms (interplay between physical forcing, biological and ecological constraints).

The multivariate representation of the ecosystem in a factorial plane founded on KW oceanic forcing also showed one state dominated the ecosystem (1983–2006), corresponding basically to an

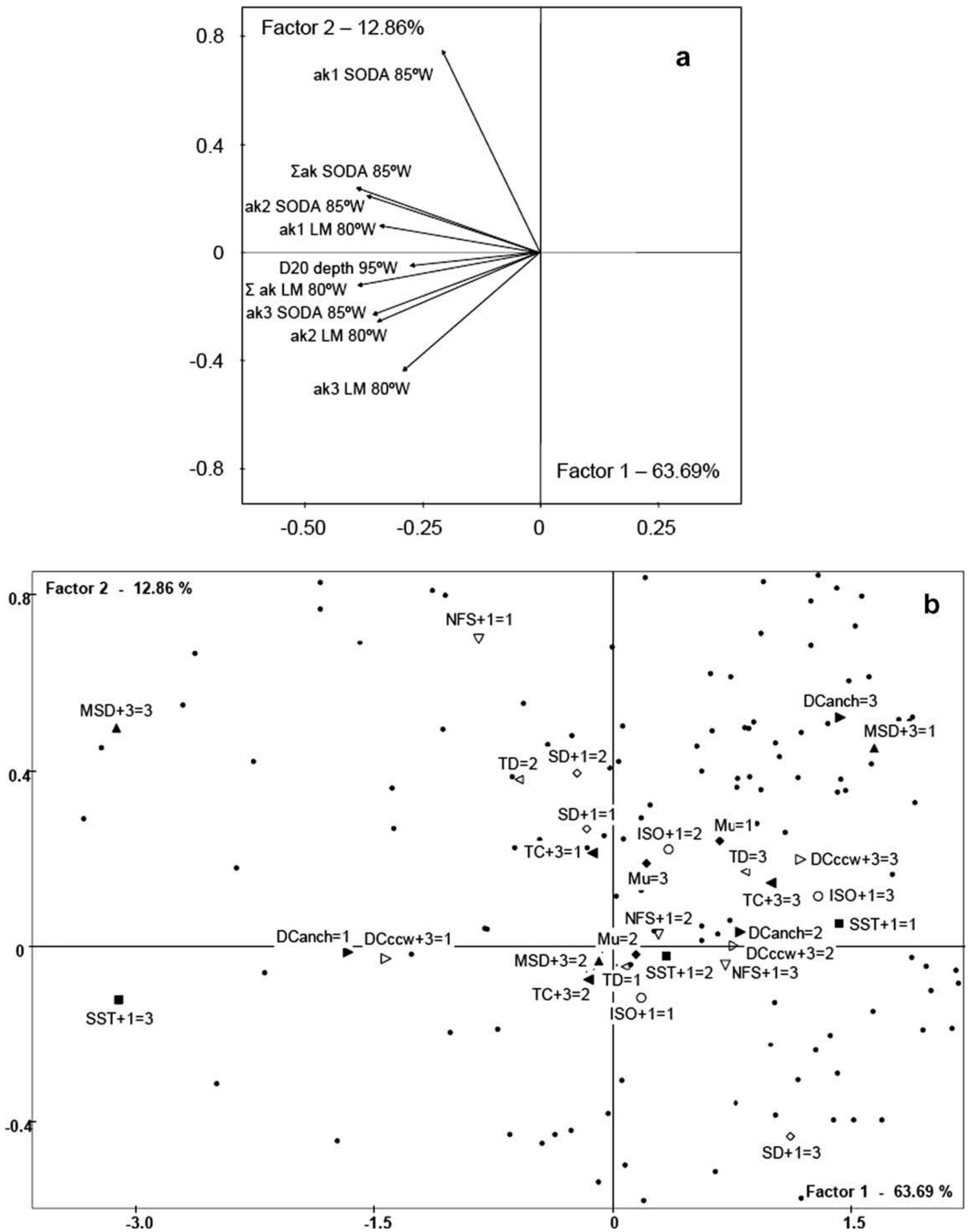

Fig. 4. Results from the PCA analysis: (a) variables describing the large scale oceanic forcing as active variables to build the multifactorial space and (b) the metrics describing the coastal ecosystem dynamics were categorised in three modalities (low = 1, medium = 2 and high = 3) and projected on this factorial plane: sea surface temperature off Chicama (SST), mean distance to the coast of the cold coastal waters (DCccw), mean depth of anchoveta schools (MSD), mean distance to the coast of anchoveta (DCanch), spatial concentration of anchoveta biomass (ISO), fishing trip mean duration (TD), fishing trip mean searching duration (SD), mean number of fishing sets by trip (NFS), mean catch by trip (TC), synthetic index of the vessels trajectories (μ).

average cold or 'upwelling dominant' scenario, with extreme trajectories corresponding to warm but punctual events (El Niño's), generated by downwelling KWs. We hypothesize that one pseudo-stable (cold and productive) state largely dominated our study period because the time series data falls (i) mainly in a cold decadal phase or 'anchovy era'; (ii) the end of a warm regime for the very first years of the time series (Alheit and Ñiquen, 2004; Gutiérrez et al., 2007) and (iii) more generally because whatever is the decadal context (warm or cool), temperature anomalies associated La Niña events (temperature anomaly for Niño 3.4 usually less than 2.5 °C) are on average less than for El Niño events, (temperature anomaly for Niño 3.4 usually less than 4 °C). It would be interesting to extend the multivariate description of the ecosystem to the different Viejo-Vieja decadal periods and anchovy–sardine alternative eras (Chavez et al., 2003). We could then test if during warm decadal periods, upwelling KWs would induce 'cold' events within background warm conditions (see also An, 2004). Additionally, other descriptors could be added in the future to this analysis, such

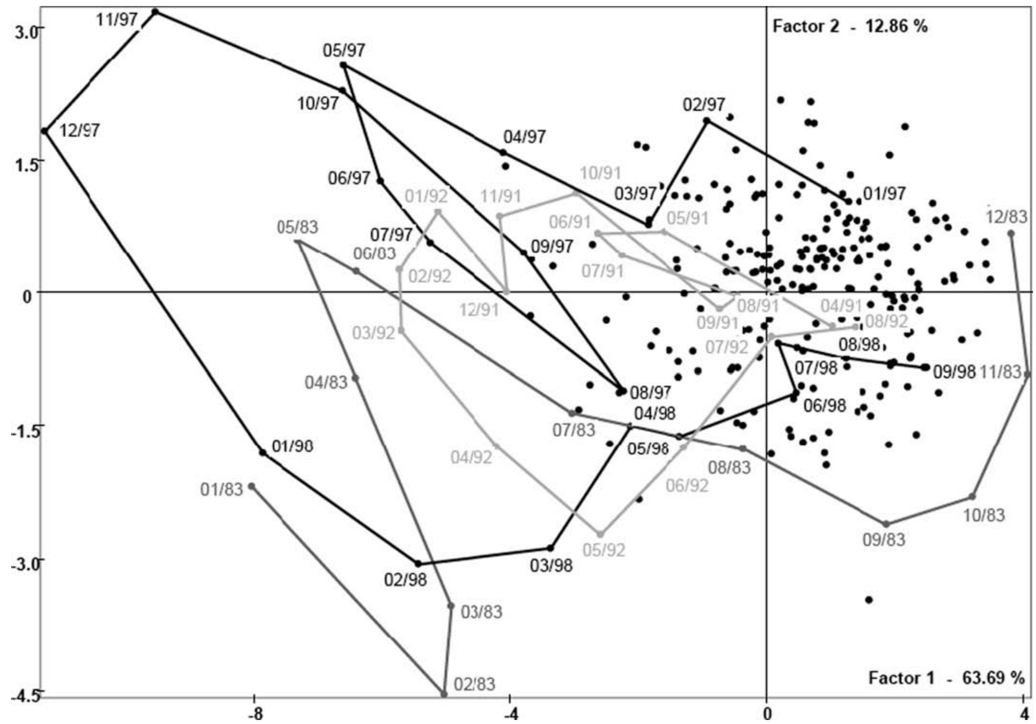

Fig. 5. Projection of the scores for each study month on the first factorial plan. The systemic trajectory for three extreme events in the ecosystem is indicated: El Niño 82–83 (dark grey), El Niño 91–92 (light grey), El Niño 97–98 (black).

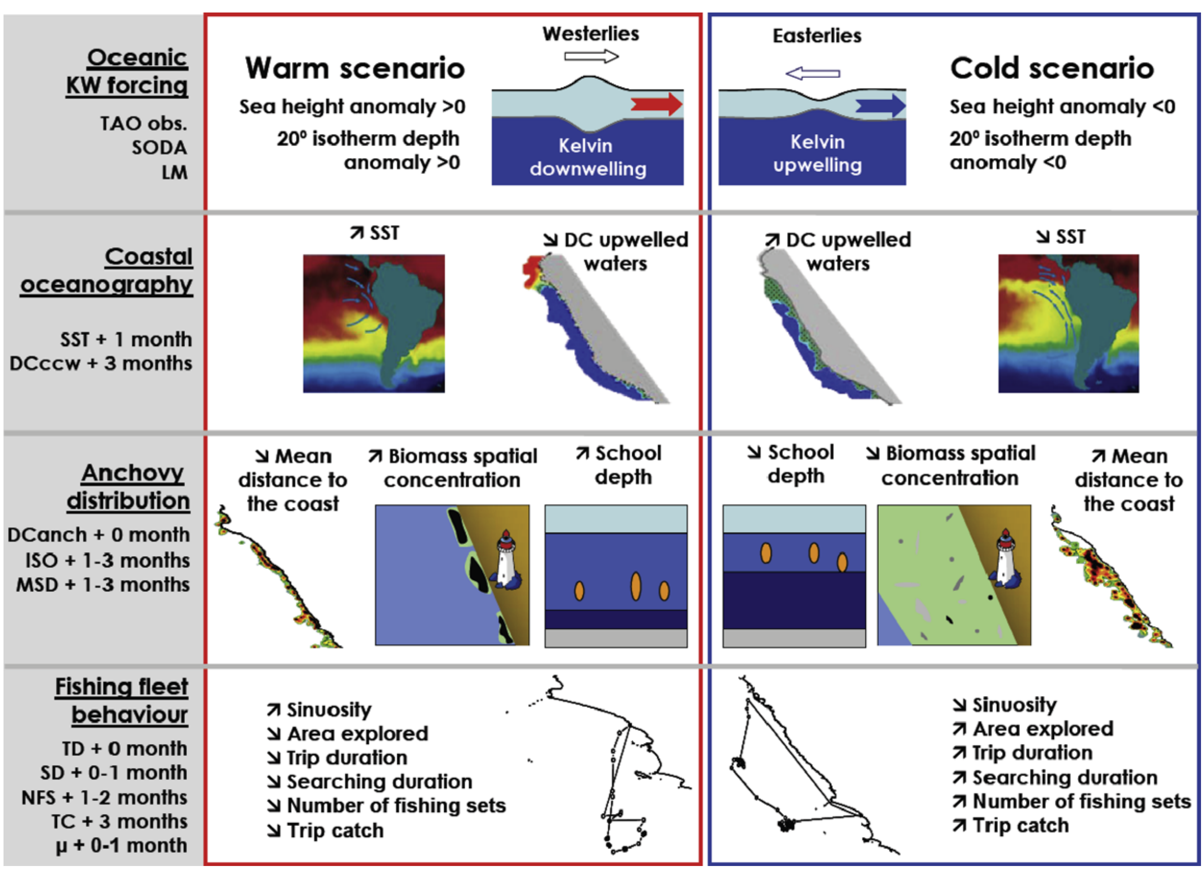

Fig. 6. Synthesis of the warm and cold ecological scenarios driven by oceanic KW forcing observed in the coastal Humboldt Current system. The qualitative response of the metrics describing the coastal ecosystem dynamics are presented for (i) Peruvian coastal oceanography: sea surface temperature (SST), mean distance to the coast of the cold coastal waters (DCccw); (ii) anchoveta distribution: mean distance to the coast (DCanch), index of anchoveta spatial distribution (ISO), mean depth of the schools (MSD); (iii) fishing fleet behaviour: mean travel duration (TD), mean searching duration (SD), mean number of fishing sets (NFS), mean trip catch (TC), synthetic index of fishing trip trajectories (μ).

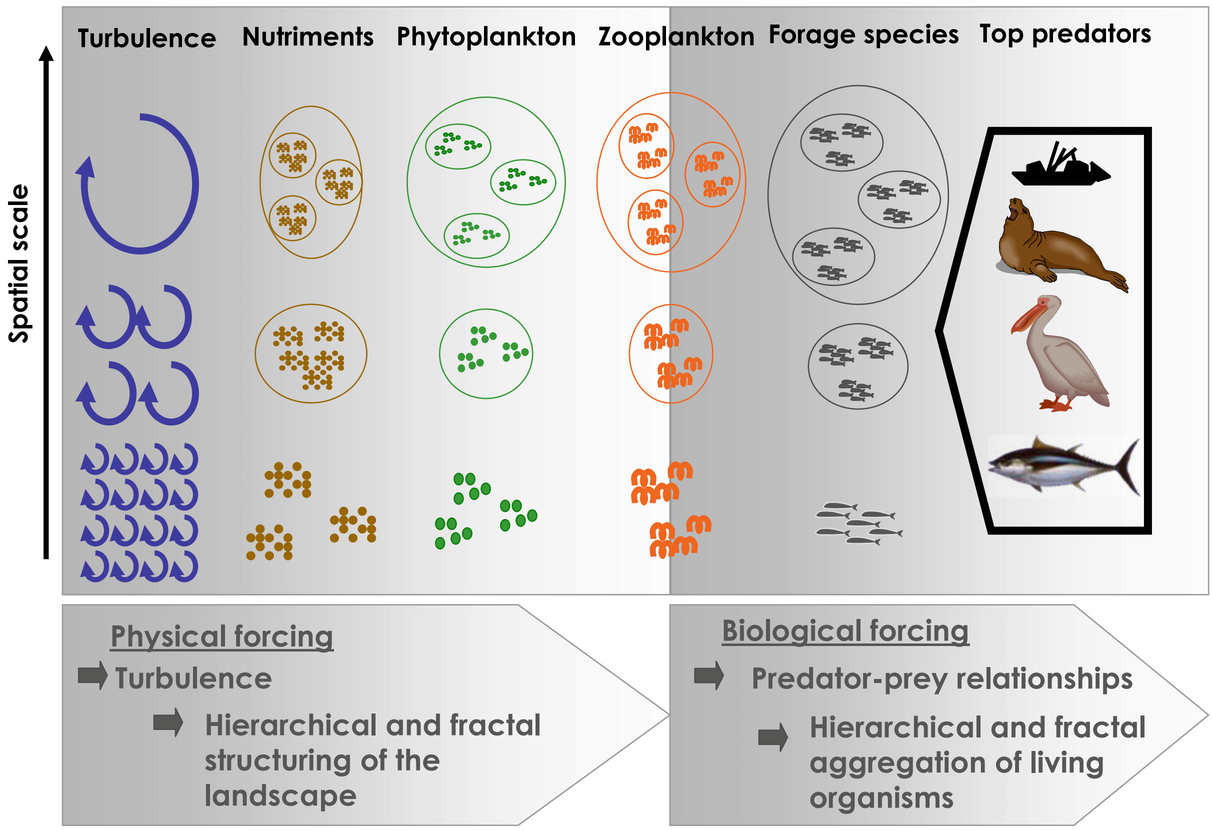

Fig. 7. Schematic representation of the concept of bottom-up transfer of behavious and spatial structuring. The physical forcing structures the pelagic landscape by introducing turbulence in the water mass. The dissipation of this turbulence is fractal by nature and generates a hierarchical structuring of the water mass. The inert particles (nutriments) and part of living organisms (phytoplankton and most of the zooplankton) are passively organized in space by this physical forcing. Then, biological interactions such as predator–prey relationships transmit to a certain extent this spatial structuring along the trophic chain.

as oxycline depth or plankton community or top predator abundances. Using a similar methodology with three decades-long study period, Link et al. (2002) produced a powerful representation of three ecosystem scenarios for the Northeast US continental shelf. As emphasized by Link et al. (2002), if fisheries managers can be more informed of overall ecosystem status they will be empowered to better make operational predictions regarding fluctuations of the resources they are charged with protecting (Pitcher, 2001).

The statistics also showed the existence of a delay between KW signal and coastal ecosystem response. The Eastern Time series that characterized KWs are located on the Equator at 85–90°W. KWs reach and pass along the Peruvian coast from this longitude in less than a week, depending on the relative contribution of the baroclinic modes ($\sim$240 km day^{-1} for the ak1 mode). However, the effects of such KWs remain strong in the Peruvian ecosystem over the next 1–3 months. The existence of these lags may be partly explained by the meso-scale effects of mixing and diffusion mentioned above, or by a ‘biological’ delay, with the biological system responding over time. However, the details of these lags remain difficult to understand. Lags were not longer for fishing activities than for fish distribution or local physical measures (Fig. 6). For instance, anchoveta reacted (in terms of mean distance to the coast) to a warm event even before that the water masses redistribution was detected (lag 0 for DCanch, 3 months lag for DCccw). If this is not an artifact of the analysis (monthly discretization of the time series, averaging data over the entire Peruvian coast), it may suggest that the KW signal is detected by organisms before the oceanography was substantially impacted or observable (see McFarlane et al., 2000).

Fishery managers need to forecast dynamics of the coastal ecosystem (e.g. Broad et al., 2002). KWs predictably affect coastal processes even when measured 2–6 months in advance in the central Pacific (see western KW time series). The detection of a downwelling KW for instance should be considered as a warning signal of forthcoming adverse conditions for anchoveta (reduced habitat and high vulnerability to the fishing fleet) and fisheries managers should then be prepared to decide temporary management measures reducing fishing pressure (closure or other). This is a piece of answer to Clark who stated as early as 1976 that “to manage the anchoveta stock properly under all the environmental conditions that occur in Peru, particularly during El Niño events, the Peruvian authorities would need to be able to predict environmental changes and their effects on the stock. Variations in upwelling strength along the coast of Peru result from large scale changes across the Pacific Ocean, and may soon be predictable from leading indicators (...)”. Not so soon, but thirty years later, we are finally able to propose that KWs amplitude (direct observations and model-resolved baroclinic modes) should be used in the dashboard of the Peruvian fishery adaptive management. Taking into account this large scale oceanic forcing signal should provide a few precious months of anticipation - months indispensable in the decision making process to make anchoveta fishery sustainable.

Acknowledgements

The authors strongly thank the Instituto del Mar del Peru (IMARPE) for having facilitated the use of the data for this work and the SODA team for making available the assimilation products that were used in this study. TAO data Project Office (NOAA/Pacific

Marine Environmental Laboratory 7600 Sand Point Way NE Seattle, WA 98115) is also acknowledged for making available on their website (http://www.pmel.noaa.gov/tao/data_deliv/deliv.html) the D20 depth data. We are also very grateful to Matthieu Lengaigne (IRD – LOCEAN laboratory) for his help in analysing and interpreting these TAO data and for fruitful conversations on this paper. This work is a contribution of the UR 097 'ECO-UP', the UMR 'LEGOS' and the Interdepartmental Thematic Action "Humboldt Current System" from IRD. This work was supported in part by the US National Science Foundation in a grant number NSF0526392 to one of the investigators (Sophie Bertrand).

References

Alheit, J., Ñiquen, M., 2004. Regime shifts in the Humboldt current ecosystem. Progress in Oceanography 60, 201–222.

An, S.I., 2004. Interdecadal changes in the El Niño–La Niña asymmetry. Geophysical Research Letters 31, L23210. doi: 10. 1029/2004GL021699.

Arntz, W.E., Fahrbach, E., 1996. El Niño: experimento climático de la naturaleza. Fondo de Cultura Económica, Mexico City. 312 pp.

Barber, R.T., Chavez, F.P., 1983. Biological consequences of El Niño. Science 222, 1203–1210.

Benjamini, Y., Hochberg, Y., 1995. Controlling the false discovery rate: a practical and powerful approach to multiple testing. Journal of the Royal Statistical Society B 57, 289–300.

Bertrand, A., Barbieri, M.A., Córdova, J., Hernández, C., Gómez, F., Leiva, F., 2004a. Diel vertical behaviour, predator–prey relationships, and occupation of space by jack mackerel (*Trachurus murphyi*) off Chile. ICES Journal of Marine Science 61, 1105–1112.

Bertrand, A., Segura, M., Gutierrez, M., Vasquez, L., 2004b. From small-scale habitat loopholes to decadal cycles: a habitat-based hypothesis explaining fluctuation in pelagic fish populations off Peru. Fish and Fisheries 5, 296–316.

Bertrand, S., Diaz, E., Ñiquen, M., 2004c. Interactions between fish and fisher's spatial distribution and behaviour: an empirical study of the anchovy (*Engraulis ringens*) fishery of Peru. ICES Journal of Marine Science 61, 1127–1136.

Bertrand, S., Burgos, J.M., Gerlotto, F., Atiquipa, J., 2005. Lévy trajectories of Peruvian purse-seiners as an indicator of the spatial distribution of anchovy (*Engraulis ringens*). ICES Journal of Marine Science 62, 477–482.

Bertrand, S., Bertrand, A., Guevara-Carrasco, R., Gerlotto, F., 2007. Scale invariant movements of fishermen: the same foraging strategy as natural predators. Ecological Applications 17, 331–337.

Bertrand, A., Gerlotto, F., Bertrand, S., Gutiérrez, M., Alza, L., Chipollini, A., Diaz, E., Espinoza, P., Ledesma, J., Quesquén, R., Peraltilla, S., Chavez, F., 2008. Aggregation behaviour and environmental forcing as determinisms of fish 3D spatiotemporal distribution across scales: the case for the anchoveta, *Engraulis ringens*. Progress in Oceanography.

Broad, K., Pfaff, S.P., Glantz, M.H., 2002. Effective and equitable dissemination of seasonal to interannual climate forecasts: policy implications from the Peruvian fishery during El Niño 1997–98. Climatic Change 54, 415–438.

Burkett, V.R., Wilcox, D.A., Stottlemyer, R., Barrowa, W., Fagre, D., Baron, J., Price, J., Nielsen, J.L., Allen, C.D., Peterson, D.L., Ruggerone, G., Doyle, T., 2005. Nonlinear dynamics in ecosystem response to climatic change: case studies and policy implications. Ecological complexity 2, 357–394.

Cane, M.A., Sarachick, E.S., 1976. Forced baroclinic ocean motions, I: The linear equatorial unbounded case. Journal of Marine Research 34, 629–665.

Carton, J.A., Chepurin, G., Cao, X., 2000. A simple ocean data assimilation analysis of the global upper ocean 1950–95. Part I: Methodology. Journal of Physical Oceanography 30, 294–309.

Carton, J.A., Giese, B.S., 2008. A reanalysis of ocean climate using Simple Ocean Data Assimilation (SODA). Monthly Weather Review 136 (8), 2999–3017.

Clark, W.G., 1976. The lessons of the Peruvian anchovy fishery. California Cooperative Oceanic Fisheries Investigations Reports XIX, pp. 57–63.

Clarke, A.J., 1983. The reflection of equatorial waves from oceanic boundaries. Journal of Physical Oceanography 13, 1183–1207.

Clarke, A.J., 1992. Low-frequency reflection from a nonmeridional eastern ocean boundary and the use of coastal sea level to monitor eastern Pacific equatorial Kelvin waves. Journal of Physical Oceanography 22, 163–183.

Chavez, F.P., Ryan, J., Lluch-Cota, S.E., Ñiquen, M., 2003. From anchovies to sardines and back: multidecadal change in the Pacific Ocean. Science 299, 217–221.

Chelton, D.B., 1984. Commentary: short-term climatic variability in the Northeast Pacific Ocean. In: Pearcy, W. (Ed.), The Influence of Ocean Conditions on the Production of Salmonids in the North Pacific. Oregon State University Press, Corvallis, Oregon, pp. 87–99.

Cotté, C., Simard, Y., 2005. Formation of dense krill patches under tidal forcing at whale feeding hot spots in the St. Lawrence Estuary. Marine Ecology Progress Series 288, 199–210.

Croll, D.A., Marinovic, B., Benson, S., Chavez, F.P., Black, N., Ternullo, R., Tershy, B.R., 2005. From wind to whales: trophic links in a coastal upwelling system. Marine Ecology Progress Series 289, 117–130.

Delcroix, T., Dewitte, B., duPenhoat, Y., Masia, F., Picaut, J., 2000. Equatorial waves and warm pool displacement during the 1992–1998 El Niño events: observation and modelling. Journal of Geophysical Research 105, 26045–26062.

Dewitte, B., Reverdin, G., Maes, C., 1999. Vertical structure of an OGCM simulation of the equatorial Pacific Ocean in 1985–1994. Journal of Physical Oceanography 29, 1542–1570.

Dewitte, B., Gushchina, D., duPenhoat, Y., Lakeev, S., 2002. On the importance of subsurface variability for ENSO simulation and prediction with intermediate coupled models of the Tropical Pacific: a case study for the 1997–1998 El Niño. Geophysical Research Letters 29 (14). Art. No. 1666.

Dewitte, B., Illig, S., Parent, L., duPenhoat, Y., Gourdeau, L., Verron, J., 2003. Tropical Pacific baroclinic mode contribution and associated long waves for the 1994–1999 period from an assimilation experiment with altimetric data. Journal of Geophysical Research 108 (C4), 3121–3138.

Edwards, M., Richardson, A.J., 2004. Impact of climate change on marine pelagic phenology and trophic mismatch. Nature 430, 881–884.

Escribano, R., Daneria, G., Farías, L., Gallardoa, V.A., González, H.E., Gutiérrez, D., Lange, C.B., Morales, C.E., Pizarro, O., Ulloa, O., Braun, M., 2004. Biological and chemical consequences of the 1997–98 El Niño in the Chilean coastal upwelling system: a synthesis. Deep Sea Research II 51, 2389–2411.

Foote, K.G., Knudsen, H.P., Vestnes, D.N., MacLennan, D.N., Simmonds, E.J., 1987. Calibration of acoustic instruments for fish density estimation: a practical guide. ICES Cooperative Research Report No. 144.

Fossheim, M., Zhou, M., Tande, K.S., Pedersen, O.-P., Zhu, Y., Edvardsen, A., 2005. Interactions between biological and environmental structures along the coast of northern Norway. Marine Ecology Progress Series 300, 147–158.

Frontier, S., Pichod-Viale, D., Leprêtre, A., Davoult, D., Luczak, C., 2004. Ecosystèmes. Dunod, Paris. 550 pp.

Frontier, S., 1987. Applications of fractal theory to ecology. In: Legendre, P., Legendre, L. (Eds.), Developments in Numerical Ecology. Springer-Verlag, Berlin, pp. 335–378.

Gutiérrez, M., Swartzman, G., Bertrand, A., Bertrand, S., 2007. Anchovy and sardine spatial dynamics and aggregation patterns in the Humboldt Current ecosystem, Peru, from 1983–2003. Fisheries Oceanography 16, 155–168.

Hsieh, C.-H., Glaser, S.M., Lucas, A.J., Sugihara, G., 2005. Distinguishing random environmental fluctuations from ecological catastrophes for the North Pacific Ocean. Nature 435, 336–340.

Keitt, T.H., Bjørnstad, O.N., Dixon, P.M., Citron-Pousty, S., 2002. Accounting for spatial pattern when modelling organism–environment interactions. Ecography 25, 155–168.

Knowlton, N., 2004. Multiple "stable" states and the conservation of marine ecosystems. Progress in Oceanography 60, 387–396.

Lebart, L., Morineau, A., Prion, M., 2000. Statistique Exploratoire Multidimensionnelle, third ed. Dunod, Paris. 439 pp.

Lehodey, P., Alheit, J., Barange, M., Baumgartner, T., Beaugrand, G., Drinkwater, K., Fromentin, J.-M., Hare, S.R., Ottersen, G., Perry, R.I., Roy, C., van der Lingen, C.D., Werneri, F., 2006. Climate variability, fish, and fisheries. Journal of Climate 19, 509–530.

Link, J.S., Brodziak, J.K.T., Edwards, S.F., Overholtz, W.J., Mountain, D., Jossi, J.W., Smith, T.D., Fogarty, M.J., 2002. Marine ecosystem assessment in a fisheries management context. Canadian Journal of Fisheries and Aquatic Sciences 59, 1429–1440.

Margalef, R., 1979. The organization of space. Oïkos 33, 152–159.

McFarlane, G.A., King, J.K., Beamish, R.J., 2000. Have there been recent changes in climate? Ask the fish. Progress in Oceanography 47, 147–169.

McPhaden, M., 1999. Genesis and evolution of the 1997–98 El-Niño. Science 283, 950–954.

Morel, G.Y., Darr, D.S., Talendier, C., 2007. Possible sources driving the potential vorticity structure and long-wave instability of coastal upwelling and downwelling currents. Journal of Physical Oceanography 36, 875–896.

Perry, A.L., Low, P.J., Ellis, J.R., Reynolds, J.D., 2005. Climate change and distribution shifts in marine fishes. Science 308, 1912–1915.

Pitcher, T.J., 2001. Fisheries managed to rebuild ecosystems? Reconstructing the past to salvage the future. Ecological Applications 11, 601–617.

Pizarro, O., Clarke, A.J., Van Gorder, S., 2001. El Niño sea level and currents along the South American coast: comparison of observations with theory. Journal of Physical Oceanography 31, 1891–1903.

Pyper, B.J., Peterman, R.M., 1998. Comparison of methods to account for autocorrelation in correlation analysis of fish data. Canadian Journal of Fisheries and Aquatic Sciences 55, 2127–2140.

Russel, R.W., Hunt, G.L., Coyle, O.K., Cooney, R.T., 1992. Foraging in a fractal environment: spatial patterns in a marine predator–prey system. Landscape Ecology 7, 195–209.

Stenseth, N.C., Mysterud, A., Ottersen, G., Hurrell, J.W., Chan, K.-S., Lima, M., 2002. Ecological effects of climate fluctuations. Science 297, 1292–1296.

Swartzman, G., Bertrand, A., Gutiérrez, M., Bertrand, S., Vasquez, L., 2008. The relationship of anchovy and sardine to water masses in the Peruvian Humboldt Current System from 1983–2005. Progress in Oceanography 79, 228–237.

Walther, G.-R., Post, E., Convey, P., Menzel, A., Parmesan, C., Beebee, T.J.C., Fromentin, J.-M., Hoegh-Guldberg, O., Bairlein, F., 2002. Ecological responses to recent climate change. Nature 416, 389–395.

Worm, B., Myers, R.A., 2004. Managing fisheries in a changing climate. Nature 429, 15.